REMARKS

The Office Action has maintained the restriction requirement and has alleged that the subject matter of Claims 108-110 are directed to a separate invention than the subject matter of Claim 67. It has thus withdrawn Claims 108-110 from consideration. The only claim examined in the present application is Claim 67.

Claim 67 was rejected under 35 U.S.C. §102(b) as defining subject matter, which is allegedly anticipated by the teachings in U.S. Patent No. 5,830,327 to Iijima.

Applicants submit the following Remarks, which are deemed to place the present case in condition for allowance. Favorable action is respectfully requested.

At the outset, before addressing the issues raised in the Office Action, it is to be noted that Iijima is not an inventor of U.S. Patent No. 5,830,327, cited in the Official Action. He is, however, a named inventor of U.S. Patent No. 5,830,326. Thus, it is assumed, for purposes of this Response, that the Official Action is referring to U.S. Patent No. 5,830,326 to Iijima ("Iijima"). Clarification is respectfully requested.

Iijima is directed to a graphite filament having carbon as a basic structural unit, which has a tubular shape being formed as a helical structure with an outer diameter of 30 nm or less. As described in column 2, line 67 to column 3, line 4 of Iijima, the tubular structure comprises multiple structures with each tubule having a helical structure. As further described in column 3, lines 28-43, the graphite filaments described therein comprise concentric nested tubules arranged to form a few atomic layers of graphite sheets making up tubular lattices, a1, a2..., shown in Fig. 2. As described in column 4, lines 25-35, utilizing the method described therein for making the product, the structure of the multiple tubular structure formed is as shown in Fig. 2. As described therein, Figure 2 shows several, **not two,** tubular lattices or graphite

sheets, a1 to a3. Although Iijima admits that it is possible to obtain a multiple structure with two, five or seven tubules and although Iijima does not indicate the amount of each tubule formed, it is apparent that the majority of the product formed does not have two layers; otherwise he would not make comments that the structure obtained from the process is as depicted in Fig. 2 which has more than two layers. Nor would he make a statement that **it is possible** to obtain a structure with two, five or seven tubules.

In fact, the product produced in Iijima is well studied and documented. The product formed by the process in Iijima, i.e., the non-catalytic (without metal catalyst added) arc process produces multi-walled carbon nanotubes with the range of tube diameters spanning from 5 nm to 90 nm, and with most of tubes having diameters between 10 and 20 nm. The diameter distribution of these multi-walled nanotubes peaks at ~ 14 nm under arc conditions that are very close to the conditions used by Iijima. See the picture with this distribution attached below (Figure 1). Under different conditions, the distribution may become narrower or wider, but the most probable tube diameter remains the same, about 14 nm. It is seen from this picture that the amount of tubes having a diameter less than ~5 nm is less than ~ 1% of the total number of tubes observed. This means that amount of carbon in double-walled nanotubes is much less than 0.1% of the total amount of carbon in other multi-wall nanotubes produced in the Iijima's synthesis, and thus any double walled nanotubes that may have been formed would not be separated from the solids produced.

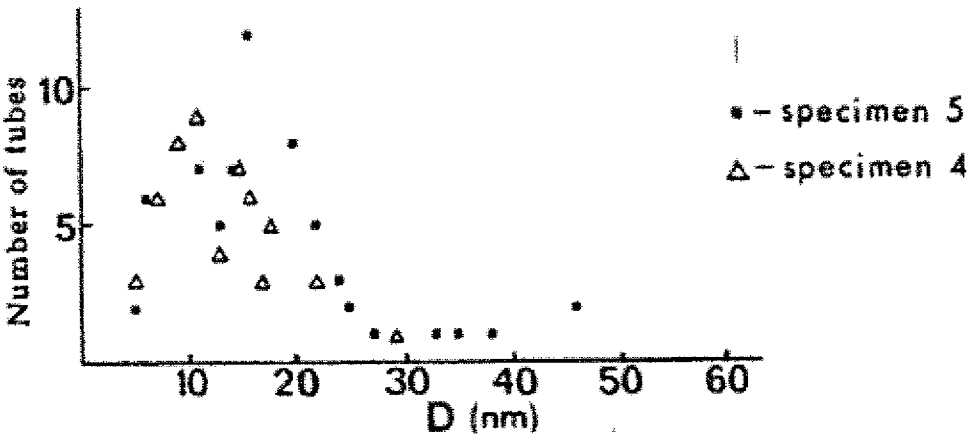

Figure 1. Diameter distribution of nanotubes produced in the non-catalytic arc synthesis under conditions close to conditions used by Iijima's US 5,830,326. From: N.A.Kiselev, A.P.Moravsky, A.B.Ormont, D.N.Zakharov, Carbon, v.37, pp.1093-1103 (1999) " SEM and HREM Study of the Internal Structure of Nanotube Rich Carbon Arc Cathodic Deposits" (See full paper attached for reference).

Nowhere does Iijima state that the predominant product is a double walled nanotube. Further, Iijima does not discuss separation of the various products formed.

The Office Action refers to Figure 2 and column 4, lines 15-35 of Iijima, alleging that Iijima discloses nanotubes having two double layers, at least a1 and a2 of carbon atoms.

Claim 67 is directed to a solid substance comprised by more than half by weight of hollow carbon nanotubes having walls consisting essentially of two layers of carbon atoms, said nanotubes consisting of two concentric nearly cylindrical graphene layers.

Applicants respectfully submit that the present invention is not anticipated by the teachings in Iijima. Case law has held that anticipation requires that the prior art reference teach and disclose each and every element of the claim, either implicitly or explicitly. MGH2/Biophile Int'l Corp. v. Milgraum, 192 F3d. 1362, 1365, 52 USPQ2d, 1303, 1305 (Fed. Cir. 1999). The absence in the prior art of any element in the claim negates anticipation. Kalman v. Kimberly Clark Corp., 713 F2d 760, 771-772, 218 USPQ 781, 789 (Fed. Cir. 1988).

It is respectfully submitted that there are differences between the present invention and the graphite filaments discussed in Iijima. As described hereinabove, the majority of the products formed in Iijima are multi-walled, and not two layers, as claimed. There is no teaching of any separation of any of the products. Thus, the product in Iijima contains mostly a multi-walled layered structure, and is predominantly a solid having a multi-walled structure. There is no product depicted or described in Iijima in which a two-layered structure is separated from the multi-walled products. A product having a multi-walled structure is not the same as a product having a two-layered structure, as claimed. Consequently, Iijima does not disclose a solid comprised of more than half by weight of hollow carbon nanotubes, ...the nanotubes consisting of two concentric nearly cylindrical graphene layers.

The Office Action refers to Fig. 2 of Iijima alleging that it is a three-layer product and that consists of two layers, in support of its rejection under 35 U.S.C. §102(b).

Contrary to the allegations in the Office Action, the product produced in Iijima contains multi-walled layer. However, even if the product in Fig. 2 of Iijima is a three-layered nanotube product, it is not the same as nanotube having two layers. But as described hereinabove, it is a multi-walled structure. As described in the present application, the product claimed is a solid substance comprised by more than one half by weight of hollow carbon nanotubes having walls consisting essentially of two layers of carbon atoms, and wherein the nanotubes consists of two concentric nearly cylindrical graphene layers. On the other hand, the multi-walled structure, as described in Iijima, is not a two-layered structure. Ignoring the number of layers recited in the claims is tantamount to ignoring one of the elements of Claim 67, which is not permitted. The claim does not recite one layer or three layers or multi-layers, but states that the nanotubes consists of two concentric nearly cylindrical graphene layers. Thus, the

schematic in Fig. 2 is not a tubule consisting of two concentric nearly cylindrical graphene layers, as claimed.

In conclusion, Iijima does not teach, or disclose a solid substance comprised by more than half by weight of a hollow carbon nanotube having walls consisting essentially of two layers of carbon atoms, said nanotubes consisting of two concentric nearly cylindrical graphene layers.

Accordingly, the rejection of Claim 67 under 35 U.S.C. §102(b) is obviated; withdrawal thereof is respectfully requested.

Thus, in view of the Remarks herein, it is respectfully submitted that the present case is in condition for allowance, which action is respectfully solicited.

Respectfully submitted,

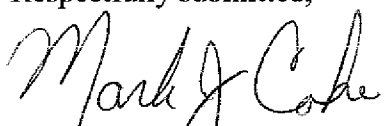

Mark J. Cohen
Registration No. 32,211

SCULLY, SCOTT, MURPHY & PRESSER, P.C.
400 Garden City Plaza, Suite 300
Garden City, NY 11530-0299
(516) 742-4343

MJC:htj

EXHIBIT A

Pergamon

Carbon 37 (1999) 1093–1103

CARBON

SEM and HREM study of the internal structure of nanotube rich carbon arc cathodic deposits

N.A. Kiselev[a], A.P. Moravsky[b], A.B. Ormont[c,*], D.N. Zakharov[a]

[a]*Institute of Crystallography RAS, Leninskii Avenue 59, Moscow, 117333, Russia*
[b]*Institute of Chemical Physics RAS, Chernogolovka, Moscow District, 142432, Russia*
[c]*Institute of Radioengineering and Electronics RAS, Mokhovaya St. 11, Moscow, 103907, Russia*

Received 28 October 1998; accepted 3 November 1998

Abstract

The structural components and the internal organization of carbon cathodic deposits fabricated using an arc with the conditions adjusted for the effective production of nanotubes have been characterized by transmission electron microscopy (TEM), high resolution electron microscopy (HREM) and scanning electron microscopy (SEM). Typically, such deposits are columnar structures oriented along the growth direction. Three main components were observed: multiwalled nanotubes, multilayer polyhedral particles and curved graphitic formations. The measured distributions and relative quantities of the components depended on the deposition regimes. Column interiors were composed of a mixture of all these components, while the outer covering of the columns was formed predominantly of nanotubes. Multiwalled nanotubes formed a mesh-like arrangement around these columns and their growth surfaces, with smaller amounts of nanotubes present inside the columns. Nanotubes in various fragments of the deposits were mainly oriented at high angles to the deposit axes. In the column coverings, groups of tubes oriented at angles >45° to the axes were present with no sets of nanotubes or bundles aligned along the deposit axes seen. Finally, a mechanism of deposit formation is proposed in connection with the recorded data.

Keywords: A. Carbon nanotubes; B. Plasma deposition; C. Scanning electron microscopy; Transmission electron microscopy; D. Microstructure

1. Introduction

Arc-discharge cathodic deposits can be regarded as a source of multiwalled carbon nanotubes (MWNs) — a novel material of solid state science that has been identified in a number of applications, for example as efficient emitters of electrons [1,2].

Though information on the internal structure of cathodic deposits that comprise of substantial amounts of MWNs can be found in various publications [3–13], still the data from direct observations are not complete enough to understand and to solve many technological problems. These include the synthesis of uniform MWNs of a particular type, their extraction in large quantities from the deposit material, purification of the MWNs from accompanying components (graphitic particles and multi-layer polyhedral particles: MPPs), and a definitive quantitative analysis of the deposit contents.

Besides this, the internal structure of the deposit is the most descriptive source of information about the processes that take place in the arc and at the growth surface, and thus it forms the basis for theories on the mechanisms of formation of MWNs and MPPs. An improved understanding of the mechanism of nanotube growth can be attained from the data on the internal structure of the deposits versus arc characteristics.

Scanning electron microscopy (SEM) and transmission electron microscopy (TEM) are very informative techniques for the direct investigation of the internal structure and composition of a cathodic deposit. With the help of these methods, it has been established that under appropriate arc conditions for nanotube synthesis, the core of a deposit has the highly ordered structure of long (up to several mm) parallel columns of about 50 μm in diameter.

*Corresponding author. Tel.: +7-95-203-4976; fax: +7-95-203-8414.

E-mail address: ormn@mail.cplire.ru (A.B. Ormont)

0008-6223/99/$ – see front matter
PII: S0008-6223(98)00309-1

The tops of these columns, that are the growth surfaces, play an important role in the electric arc process, in particular by being (according to [6]) the principal area of electron emission into the arc plasma. It becomes clear that such details of the deposit structure as the direction of nanotube orientation should be of prime importance for understanding the nature of some macrocharacteristics of the deposit, e.g. its magnetic properties [5,13]. As the structural details are most reliably found by direct observation, SEM investigations of columns and their tops have received most of our attention in this work. The principal aim of the SEM investigations was to understand the localization and orientation of nanotubes and nanotube bundles in the deposits. Particular attention was focused on the search for sets of nanotubes that were oriented in the same direction and especially aligned along the axis of the deposit growth. In our work we used methods of sample preparation for the SEM investigations that minimized the damage to the original structure.

Nanotube aggregates and their size distributions have been explored by conventional transmission electron microscopy (TEM). The internal structures of nanotubes and MPPs have been studied in greater detail by high resolution electron microscopy (HREM).

It has been found in the present work that structures of columns and their tops are different from other reports (for example in [6]) based on either indirect data, or on SEM investigations of samples prepared by methods that can alter the original structure.

2. Experimental

2.1. Preparation of cathodic deposits

Deposits have been fabricated by the DC arc method adjusted with the help of electron microscopy to give a high yield of nanotubes. The lower vertical graphite anode was in most experiments 6 mm in diameter and 200 mm long. Thicker graphite anodes (~10 mm) were used as well. The upper stepping-motor driven graphite cathode of 15 mm in diameter was the site of a downward growing cylindrical deposit. Each run was conducted under three fixed parameters: (1) the rate of feed of the graphite rod into the arcing zone, (2) the helium pressure and (3) the arc current. Fluctuations of the latter were monitored with an oscilloscope so as to adjust the stable regime of the discharge, which has been recommended for obtaining high quality tubes [3–6]. The reaction chamber was water cooled.

These three externally controlled parameters define the values of two observed derivative parameters of the arc process, namely the gap width and the voltage drop across the gap. These parameters are interdependent (as discussed later), so that any variation of the controlled parameters changes the derivative parameters. In the present search for better technology of nanotube production it is reasonable to relate the obtained results, including the above mentioned derivative parameters, to a given set of the named three externally controlled parameters, ensuring the possibility of reproducing the attained experimental results.

Under conditions used in this work the deposits obtained had the form of cylinders 50 to 100 mm long and 5–12 mm in diameter. As it could be seen by the naked eye or in the optical microscope at low magnification, the hard outer grey shell of a cylinder enveloped a soft black fibrous core containing (according to electron microscopy studies described later) nanotubes of various forms, their aggregates, nanoparticles and various forms of graphite. The concentration of nanotubes in the core of investigated deposits depended on the deposition conditions and varied over a wide range from almost entirely absent (several tubes or their bundles in the SEM field of view ~25 μm^2 in size) up to the level where some regions of deposits consisted predominantly of tubes (~100–200 tubes in the same field of view).

Both untreated cathodic deposits (in preference) and deposits subjected to oxidation in air [6] and/or acid solutions of potassium permanganate [7] were investigated. The oxidation processing was aimed at increasing the nanotube concentration in the deposits through the removal of other components, which can otherwise hide the tubes from view.

2.2. Electron microscopy measurements

Specimens for TEM and HREM were prepared by dispersing the core parts of deposits in acetone by using an ultrasonic bath. A drop of the suspension was put on a lacy carbon film supported by a copper grid. Specimens were investigated in a Philips EM-430ST electron microscope operated at 200 or 250 keV, and in a Jeol JEM 4000EX microscope operated at 400 keV. Several tens of low magnification micrographs of each specimen were made for semiquantitative characterization of a deposit. The most typical structural components were investigated further by HREM in phase contrast mode at a point-to-point resolution ~0.16 nm.

For SEM investigations, deposit growth surfaces, cross-sections, and randomly split-apart fragments, both as received and after oxidation treatment, were considered. They were studied at various angles by using a low-voltage Jeol JSM-840 microscope. Deposit rods were split by manually holding the sample away from the area to be investigated. Care was taken not to disturb these freshly exposed areas. Usually the appearance of cross-sections was step-like with transverse and longitudinal (with respect to the deposit axis) regions, with columnar structures clearly visible in the core of a deposit. No special attempts were made to get longitudinally split columns, as the high mechanical stresses that would be used in these cases could alter their internal structure. Samples were fixed to SEM holders with silver dotite paint applied to the samples

No sample coating was used.

The JSM-840 microscope was also operated in high resolution mode with the accelerating voltage at 12 keV and the electron beam current ~10 pA. Secondary electron images were recorded at working distances of about 15 mm. The low values of the beam current provided the necessary spatial resolution and eliminated the possibility of electron-beam modification of the samples during observation.

3. Results

3.1. HREM and TEM of deposit components

Three distinct structural components have been observed in all the investigated specimens: MWNs of the type first observed by Iijima [8], MPPs, and various kinds of graphitic particles. A HREM image of such MWNs and MPPs is shown in Fig. 1. Along with approximately isometric particles, formations intermediate of tubes and MPPs have been observed in small quantities, for example elongated particles constructed of two to four sets of conical layers. Some varieties of MPPs and MWNs seem elongated MPPs that terminate as cylindrical nanotubes. Graphitic components have been mainly found as coiled graphite ribbons (Fig. 2). The quantities of these components in the deposits as well as the tube diameters and sizes of the MPPs depend very much on the arc parameters.

The majority of investigated specimens could be divided into three groups according to the controlled parameters: (1) fabricated at different He pressures and arc currents, while keeping the linear feed velocity constant; this group is exemplified by the first three entries in Table 1 (specimens 1–3); (2) different only in feed velocity (specimens 4 and 5); (3) fabricated at high He pressures (specimens 6 and 7). Several thicker deposits ~11 mm in diameter produced with thicker graphite anodes were also prepared for structural investigations (specimen 8).

Distributions of nanotube diameters and linear sizes of isometric multilayer polyhedral particles have been found by TEM observations. Corresponding histograms are drawn in Fig. 3 and brief descriptions of sample compositions derived from TEM investigations are given in Table 1. Specimens produced at low He pressure contained small amounts of tubes. Thus the main component of specimen 1 was curved graphite (Fig. 2). The tendencies for the tube quantity to increase and for the graphitic components to decrease with the increase in He pressure and the decrease in arc current are clearly revealed by the first three examples in Table 1. This statement is confirmed by investigations of deposits obtained at higher pressures. Thus in specimen 6, the main components were tubes and

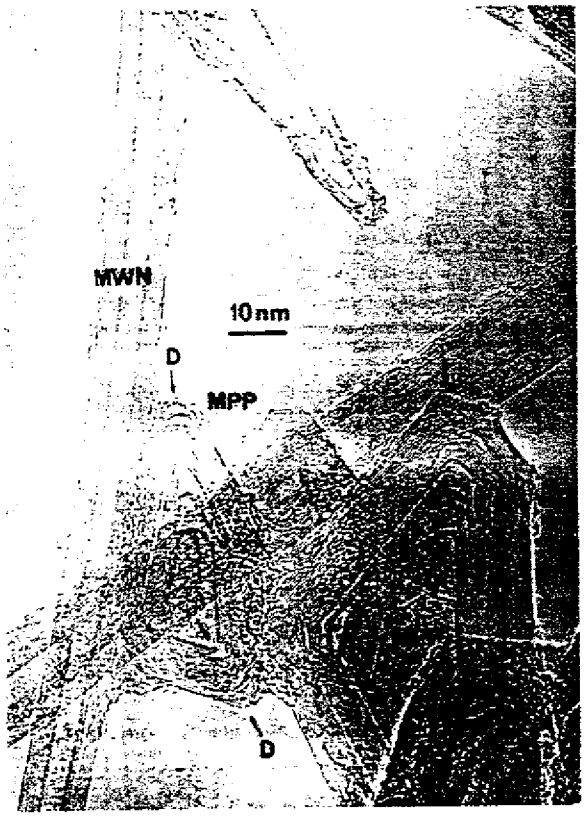

Fig. 1. HREM image (400 keV) of multilayer polyhedral particles (MPPs) and multiwalled nanotubes (MWNs). Inner cavities and defects in vertices (D) are visible. Specimen 3 (for fabrication parameters see Table 1).

Fig. 2. HREM image (400 keV) of specimen 1 that comprised of small amounts of nanotubes (MWN) and onionites (O). Curved graphite (G) was the main component of the specimen.

Table 1
Conditions and parameters of the arc process during the production of the studied deposits

Sample number	Graphite rod diameter(mm)	Deposit diameter (mm)	Helium pressure(torr[a])	Arc current(A)	Anode feed velocity(mm/min)	Gap width(mm)	Voltage drop across the gap (V)	Deposit growth rate (mg/min)	Brief description of the deposit composition derived out of the electron microscopy observations
1	6	7.8	100	80	4	3.9	18.0	115	Low tube concentration; main component — curved graphite (Fig. 2); MPPs had rounded vertices and resembled onion-like particles
2	6	6.5	200	65	4	2.2	19.0	170	More tubes and MPPs than in sample 1; tube diameters 8–22 nm, the most probable diameter — 15 nm (Fig. 3a); the size of MPPs — 20–85 nm (Fig. 3c)
3	6	7.4	700	55	4	0.5	20.8	260	The lowest amount of graphite in the group of samples 1–3; tube diameters — 8–23 nm, the most probable diameter — 12–14 nm (Fig. 3a)
4	6	8.0	500	65	8	0.4	21.3	350	Tubes 5–29 nm in diameter (Fig. 3b); MPPs 19–93 nm in size (Fig. 3d); many graphitic particles
5	6	7.6	500	65	2.5	3.5	22.3	90	Tubes 5–46 nm in diameter; the most probable diameter 14–16 nm (Fig. 3b); MPPs 9–93 nm in size, the most probable size — 27–49 nm (Fig. 3d); very low amount of graphite
6	6	5.6	1500	65	1.4	4.2	31.1	20	The main components — tubes and MPPs (Fig. 4); tube diameters — 4–60 nm, (Fig. 3a); the sizes of MPPs — 8–120 nm (Fig. 3c)
7	6	5.5	2000	65	1.4	3.3	32.1	22	Composition is close to that of sample 6. High tube concentration, MPPs and graphitic particles
8	10.6	11.3	500	160	0.65	0.8	22.4	160	Composition is close to that of sample 6. High tube concentration, MPPs and graphitic particles

[a] Pressure values in the reaction chamber during the arc operation.

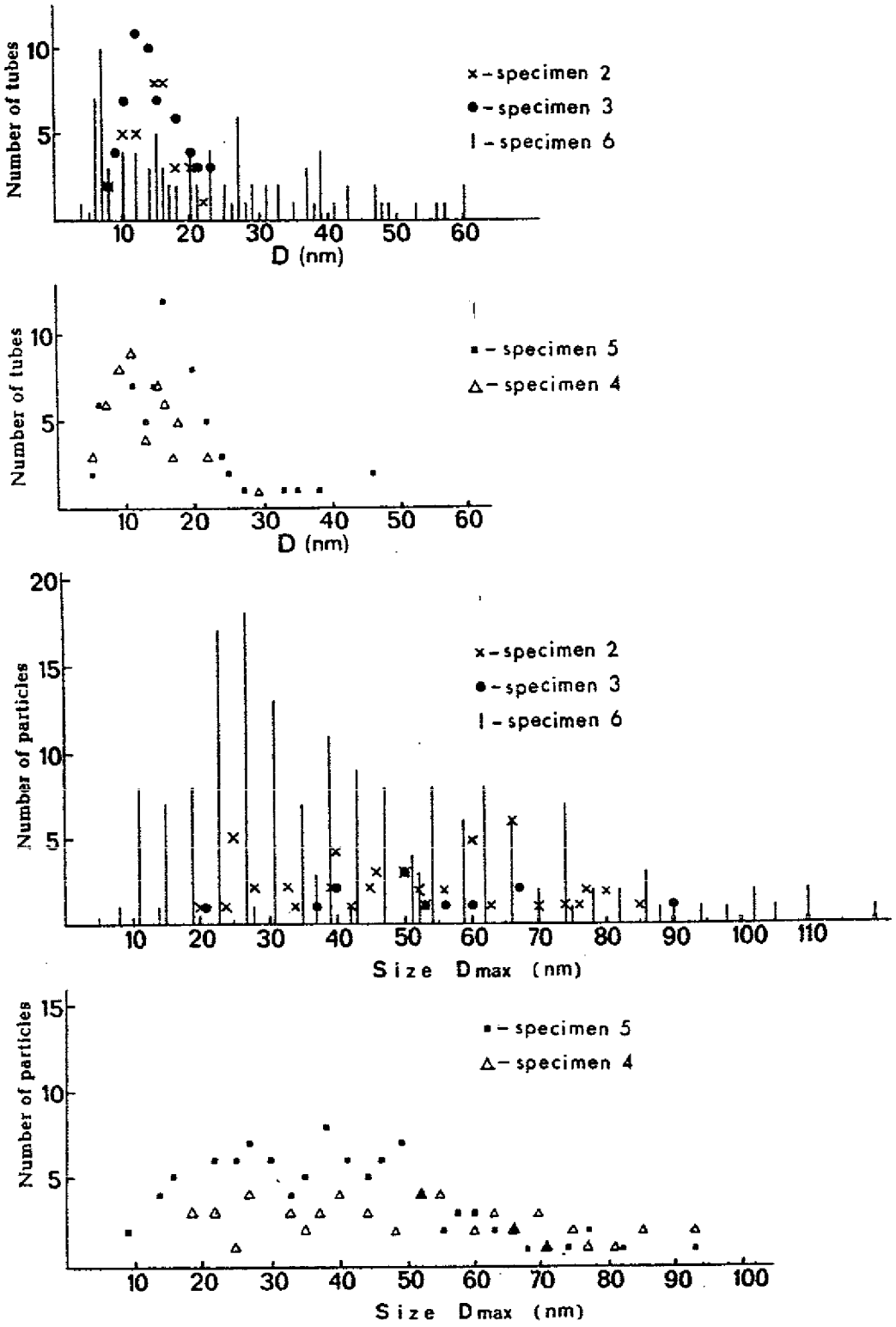

Fig. 3. Distributions of nanotube diameters (a, b) and linear sizes of isometric multilayer polyhedral particles (c, d). (Numbers of measured MWNs and MPPs for histograms are shown in parentheses).

MPPs (Fig. 4). The range of nanotube diameters (Fig. 3a) was much wider than that for specimens 1, 2 and 3. So were the sizes of the MPPs (Fig. 3c). Again we observed a much wider range compared to 1, 2 and 3 samples. Thus higher He pressures facilitate broadening of the size distributions of both the tubes and the MPPs.

The influence of the feed velocity on the composition of the deposit is exemplified by entries 4 and 5 in Table 1. At

Fig. 4. TEM image (250 keV) of specimen 6. The main components are multilayer polyhedral particles (MPPs), nanotubes (MWN) and graphite formations (G).

a feed velocity equal to 2.5 mm/min (specimen 5) we were close to its optimal value at 500 torr He pressure and 65 A arc current for 6-mm diameter graphite rods. It should be noted that at a low feed velocity (specimens 5 and 6) a wider range of nanotube diameters is prominent. Nanotubes of very small diameters, very small-sized MPPs, as well as very thick MWNs were observed. Thus lower feed velocities (wider gaps) facilitate the broadening of size distributions in a manner similar to increasing the He pressure.

It should be stressed that no sole parameter or its optimal value may be identified at present as the most crucial factor for determining the deposit's components. For example, comparable yields of MWNs can be obtained with either a narrow or wide gap-width. Actually the composition of a deposit will be dependent mainly on the temperature and carbon vapor properties inside the gap, which are determined by a multitude of factors, including He pressure, carbon arc power, graphite rod size etc. (see [14]). Therefore, at present the combined influence of all the parameters must be considered in the search for the optimal conditions of MWNs synthesis.

It would be of interest to characterize the lengths of nanotubes using histograms. This task still remains mainly because of the aggregation of the tubes. Measurements of lengths of various nanotubes encountered in deposits (though not the distributions because of tangled nanotube aggregations) have been performed with SEM.

On the basis of TEM measurements it has been possible to select nanotube rich specimens. These are represented in Table 1 by specimens 6, 7 and 8. Besides MWNs they contain MPPs and graphite. 3D organization of these components in the deposit core is also of interest. But it cannot be revealed by TEM because the sample preparation completely destroys the deposit structure. Only secondary aggregation of components will be exposed by TEM and HREM, like nanotube side-by-side bundles and large agglomerates of MPPs. SEM was the better instrument for the examination of the internal deposit structure, the localization of the main deposit components, and the exploration of the orientation of the nanotubes.

3.2. SEM investigation of the internal organization of deposits

In this section the 3D organization of the deposits is considered as revealed by SEM measurements. Nanotubes are better distinguished by the SEM compared to MPPs and similar formations, which are liable to aggregation. MPPs in SEM images were identified as the isometric particles that were ~30–100 nm in size.

In accordance with earlier reported results [4–6,9,10], the soft black core of a deposit obtained under favorable conditions for the production of nanotubes was composed of parallel columns of about 50–60 μm in diameter aligned along the axis of the deposit growth. The top growth surface of the deposit was almost flat when the optically black core was most abundant. This case corresponded to high helium pressures and low arc currents, which were preferable for a higher yield of nanotubes. An SEM top-view image of a region of the growth surface of a deposit (Fig. 5a) shows the tops of these columns forming a honeycomb-like structure. Viewing the surface at an angle of 70° to the deposit axis reveals that the tops of the columns are nearly hemispherical (Fig. 5b). The tops of adjacent hemispheres were separated by 65–75 μm, that is

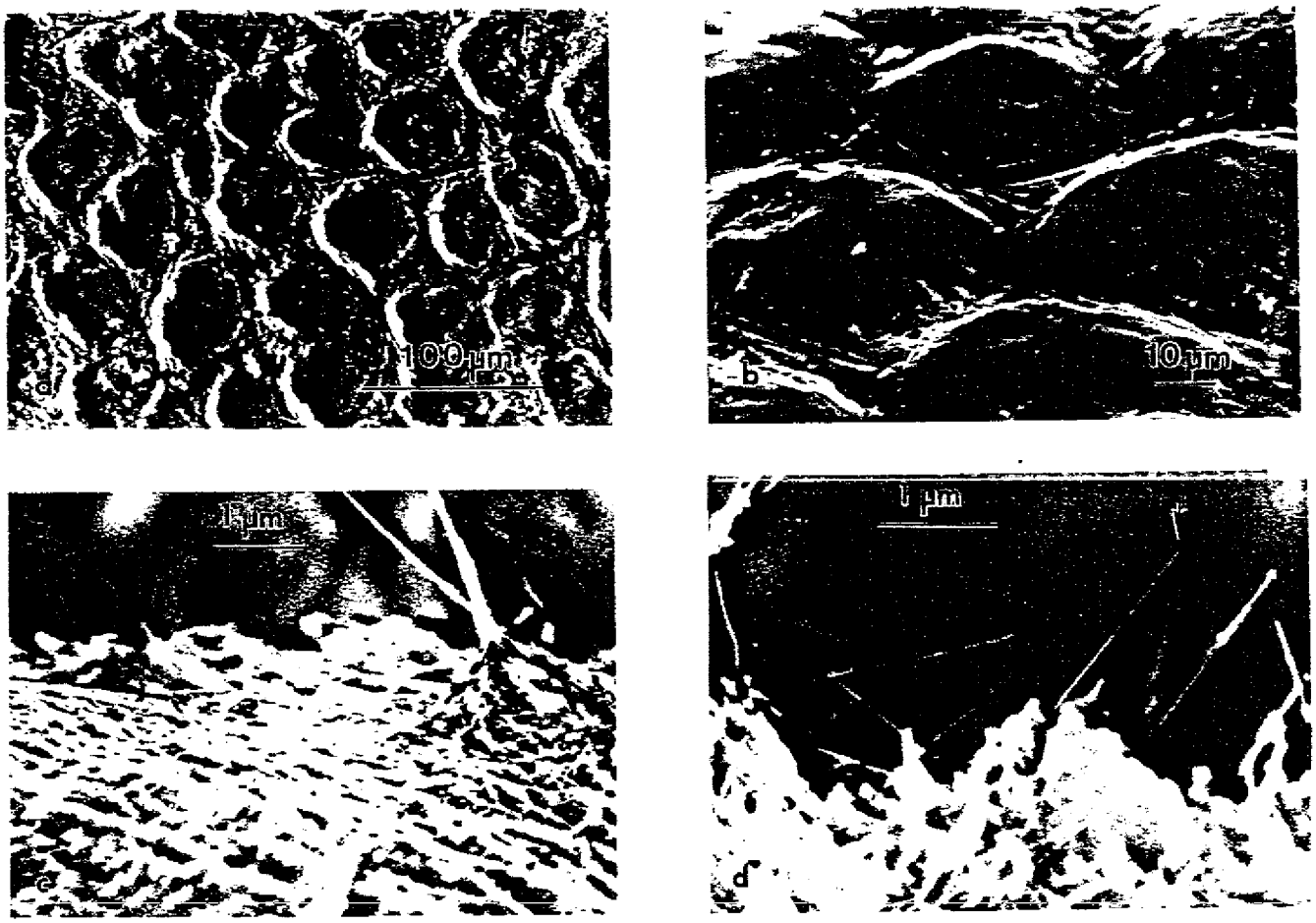

Fig. 5. SEM images of the growth surfaces of typical deposits. (a) A top view at low magnification of sample 7; (b) hemispheres at the column ends at higher magnification (side view taken at 70° to the deposit axis) of sample 7; (c) a separate hemisphere covered with nanotubes and their bundles that lie on the growth surface (side view taken at 60° to the deposit axis); sample 8 (it is characterized by higher (11.3 mm) deposit diameter then other samples, but shows similar column structure); (d) side view of the surface of a hemisphere at high magnification (taken tangential to the surface); nanotubes down to 20–30 nm in diameter and up to 4 μm long (arrowed) are clearly seen; sample 6.

substantially less than the corresponding distance reported in Ref. [6], probably because of the difference in arcing conditions. A closer examination of a separate hemisphere on the growth surface of a deposit just removed from the arc apparatus (that avoided the accidental removal of the delicate nanotubes from the surface) revealed a layer of fibers densely covering the top of the column (Fig. 5c). These fibers according to their dimensions and morphology could be like the nanotubes or their bundles seen in our TEM and HREM investigations. It is likely that such a covering layer had been the source of the MWNs discovered with the HREM by Iijima [8]. Most of the nanotubes that covered the tops of the columns lay along its upper surface or at angles exceeding 45° from the axis. In some places tubes extended from the covering layer (Fig. 5d), showing their diameters to be equal to 20–30 nm. That was consistent with the TEM data for the separate nanotubes. These protruding nanotubes led to the possibility of using separate columns several mm long as electron field emitters.

The typical cross-sectional view of a deposit also reveals the friable columnar structure of quasi-hexagonal ordering mentioned above, with distances between the column axes of about 65 μm (Fig. 6a). As seen in Fig. 6a, the appearance of the cross-sections is usually step-like with transverse and longitudinal (with respect to the deposit axis) areas. After sectioning, longitudinal areas of steps (up to ~1 mm long) always pass between columns. Some protruding columns nearest to the step edges separate at their ends making the observation of their lateral sides convenient at various angles. Sections of columns themselves were usually normal to their axes or slightly inclined to them. At a higher magnification (Fig. 6b) it is clearly seen that columns 60 μm in diameter in a given fragment are separated by a low density intercolumnar space of 10–15 μm as distinct from about 50 μm

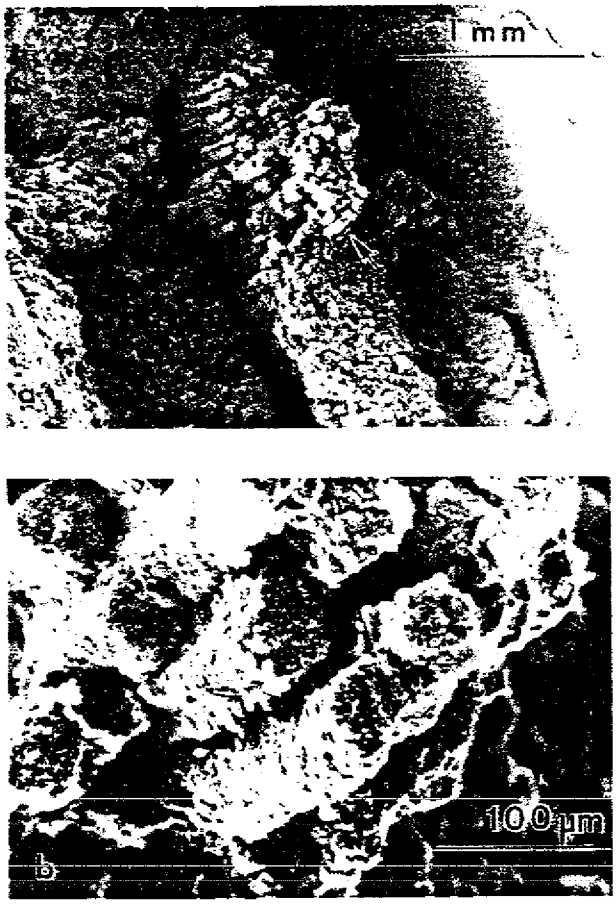

Fig. 6. SEM image of the cross-sectioned deposit (specimen 7). The growth axis is directed from the observer along the columns. (a) The columnar structure at low magnification. Friable columnar structure and dense layered structure (upper right) are seen there. Aggregates of columns with cross-sectional dimensions of about 0.5–1 mm attract attention. The arrowed area is shown in (b) at higher magnification. (b) At higher magnification the most friable area between the columns is well discernible. After splitting, some columns have separated.

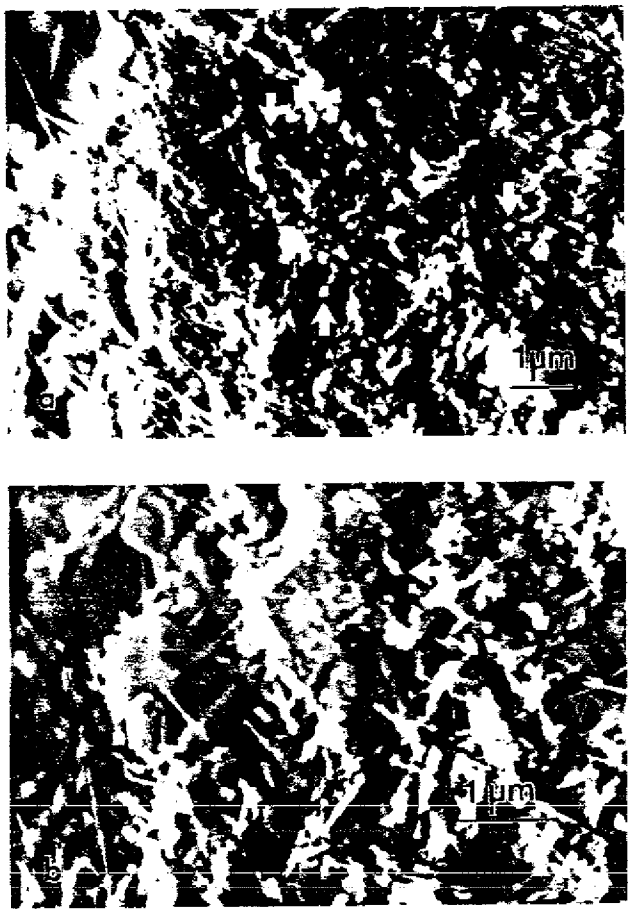

Fig. 7. SEM images of the cross-sectional view of the sectioned separate column (specimen 7): (a) near its edge (the growth axis is directed upwards and is inclined at the top of the image ~20° from the image plane). One can see the lateral braiding of nanotubes (the bright nanotube area on the left characterized by high secondary electron emission) and the internal section of the column (on the right). Inside the column there are no nanotube co-oriented structures having uniform alignment, including any structures along the column. Some spear-like tubes are directed outwards from the lateral side (the braid) of the column; (b) near the center of the column; normal view; the growth axis is directed from the observer. Particles that can be considered as MPPs are indicated with arrows.

intercolumnar spacing observed earlier [6] after the somewhat lower arc-current deposition densities. Our investigation shows that the highest concentration of nanotubes is attained in those low density intercolumn spaces and at the side surfaces of the columns. SEM examination of a cross-sectioned separate column (chosen from the cross-sectional deposit view) reveals an area of enhanced emission of secondary electrons along its circumference (Fig. 7a). This area is composed of interlaced nanotubes forming an outer braid to the column. The characteristic thickness of this (measured on protruding columns) was about several micrometres. The outer diameter of protruding columns varies along their length in a somewhat periodical manner (Fig. 6b). The inner part of a column inside the braid (to the right of the braid in Fig. 7a) consists of a disordered mesh of various forms of graphite mixed with 50–70 nm diameter MPPs and smaller amounts of nanotubes. If there had been any longitudinally

such an observation. Randomly oriented nanotubes amidst other particles were also revealed by the SEM (Fig. 7b). No tubes aligned along the deposit axis were seen in Fig. 7b and the like (they would have been observed as a collection of very bright dots). It can thus be stated that in the columnar structure of the black core, the MPPs and curved graphite particles were concentrated inside the columns. It should be noted that MPPs and graphite components were rather tightly embedded inside the columns and often overlapped each other, leaving no room for longitudinal void channels, where co-oriented long nanotubes or their bundles could be formed. No preferential co-orientation of nanotubes or their bundles was seen inside cross-sectioned columns, despite observations at

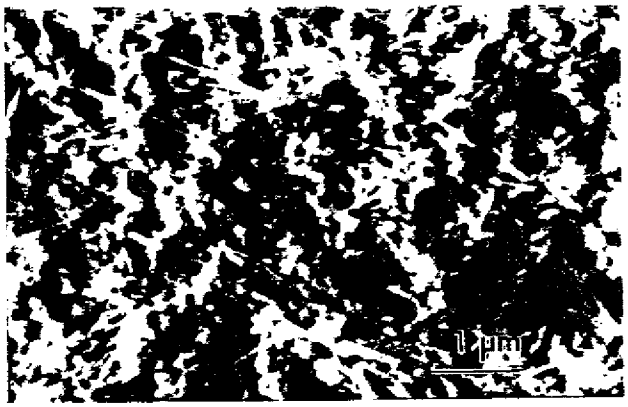

Fig. 8. Typical SEM image of the lateral side of a separate column revealing the nanotube braid and its structure (specimen 7). The direction of observation is normal to the lateral column side. Groups of tubes oriented at ~70° to the growth axis (the vertical line) are clearly visible. Few tubes are oriented close to the vertical direction, there are practically no tubes oriented perpendicularly to the growth axis.

Typical SEM image of the side surface of an intact column taken in the direction normal to column axis (Fig. 8) shows the structural organization of the outer layer of the braid. It consisted predominantly of interlaced nanotubes and their bundles. The thinnest observed tubes were 20–30 nm in diameter, that agreed with the TEM data. No significant inclusions of components other than nanotubes were observed in these outer layers. It is important to estimate the average direction of nanotubes in the braid with respect to the deposit growth axis. Analysis of column side views (about 25 μm^2 in size) has shown that in most of them, more than 50% of the nanotubes or their bundles are inclined in the micrograph plane at angles exceeding 45° relative to the deposit axis. Side images (like that shown in Fig. 8) often reveal that noticeable part

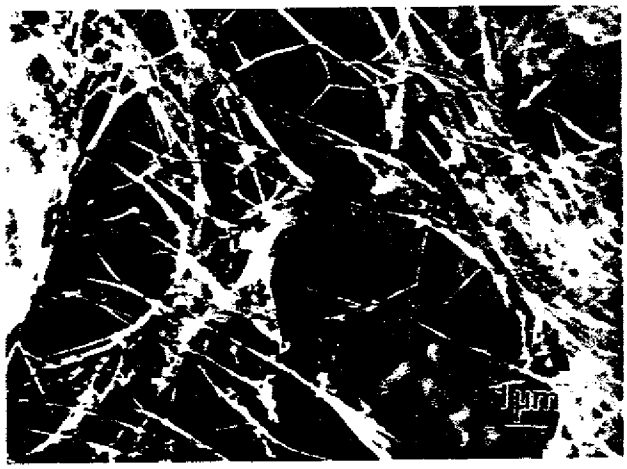

Fig. 9. SEM image of the nest-like structure of nanotube bundles found in the interspace between columns in the oxidized specimen 7.

that correspond to 45–75° relative to the axes. Many of them are tangential to columns. Few tubes lie along axes or normally to them. Thus we can conclude that nanotubes in the braid covering the columns are inclined on average more than 45° with respect to the axis of a deposit.

Oxidative etching of columnar structures in air helps to reveal (or produce) fairly pure arrays of nanotubes located in the intercolumnar space. They often form nest-like structures (Fig. 9). The thinnest nanotubes observed in the intercolumnar space (~20 nm in diameter) were protruding from the braid as spear-like tubes seen in Fig. 5d.

Though in the majority of columnar structures there was a very noticeable content of nanotubes, on the basis of our examinations it should be noted that the existence of columns in deposits does not necessarily bear evidence about high concentration of nanotubes between columns and inside them. In some deposits, the columns had a low content of nanotubes both at their peripheries and inside them. Such columns may consist predominantly of other types of carbon particles, e.g. of variously stacked graphene layers. Growth surfaces of such columnar structures are not as regular as in the case of nanotube rich deposits. Thus, the formation of columnar-like structures in deposits is a necessary condition, but not the only condition for the production of high concentration of nanotubes in deposits.

The elements of the described columnar structures are rather fractal-like. This comes out of the fact that similar SEM images are often registered at different scales. That means that small and large details of the structures are geometrically close to each other except for scale. Thus on a cross-section of a deposit at essentially low magnifications one can see (Fig. 6a) clear agglomerates of similar columns ~1 mm in diameter that resemble separate columns, and at greater magnifications inside these columns one can find spatial structural formations of composites $\leq$10 μm in diameter surrounded by nanotubes. This demonstrates the *self-similarity* [15] of the columnar 3D structures, which is the important property of fractals. The honeycomb-like column structure described above has much in common (see also Ref. [6]) with the Bénard convection cells in fluids that are fractals [16]. So nanotubes grow as an essential part of a fractal-like solid that cannot be synthesized in the linear system, but only in a complex non-linear dynamical system [15,16], which in our case is the arc plasma. This result is important for the search for better technology of nanotubes production in deposits.

4. Discussion

The reported results are in accordance with earlier electron microscopic observations of cathodic deposit structures [4–6] except the issue of the nanotubes location

and orientation in a column, denoted in Ref. [6] as zone 1. The columns are generally thought to be composed of MWNs aligned along their axes as distinct from the picture outlined above: nanotube braided columns filled with randomly oriented nanotubes, MPPs and graphite. There are several plausible reasons, which might account for the discrepancy. First is the different sample preparation procedure for SEM observations, which remains poorly defined in other papers. For example, the use of a microtome can quite easily cause the alignment of tubes along the direction of the cut, as has been the result of slicing the composite polymer resin matrix containing originally randomly dispersed nanotubes [11]. The other reason may be the intrinsic uncertainty in the actual orientation of a very thin object that is used for HREM observations, again due to the method of sample preparation for viewing a tube down its axis [5,12]. Finally, the difference in the arcing conditions can cause drastic variations in the columnar structure. Our experience rejects the latter, for we have not observed the axial orientation of nanotubes in columns in any of the numerous samples studied. Nevertheless, further SEM studies of different columns with the highest possible resolution seem pertinent.

An indirect indication of the direction of nanotube orientation in columns can be derived from deposit magnetization anisotropy measurements, which reveal that the value of longitudinal diamagnetic susceptibility for deposits is about 10% higher than the value of the transverse susceptibility [5]. Under the assumption that the longitudinal component of susceptibility dominates in a tube, the conclusion has been made that tubes must be oriented preferably along the deposit axis to explain this observed macroscopic anisotropy [5]. Quite recently it was experimentally substantiated that this assumption was incorrect [13] and that the nanotubes in the deposit investigated in Ref. [13] were preferably oriented at high angles to the deposit axis, in complete accordance with the results of the present work achieved from direct SEM observations of similar deposit samples.

The structure of the nanotube rich columns established in the present work does not correspond to the hypothesis about the alignment of tubes along the column axis, which is an essential point in a model [6] offered to describe the growth of a deposit in a direct current arc. In this model the tips of parallel nanotubes in zone 1 (top of columns) act as field emitters of electrons into the plasma. This electron injection produces a high degree of carbon ionization resulting in a carbon ion current flow concentration above columns, that provide the principal feedstock for their growth. The helium buffer gas is drawn in by the carbon ion flux to the tops of the columns and then sweeps to their sides and returns back to the plasma over zone 2, the intermediate area between adjacent columns.

Some refinement of this model seems necessary in view of data on the column structure discovered. The emission of electrons from tops of columns (zone 1) in the absence of a large amount of vertically oriented nanotubes (Fig. 5c and d) may be thought to occur as mainly thermionic in its nature from all the constituents of columns, at the same time keeping the possibility for the occurrence of the field emission from inclined nanotube tips and sharp edges of other particles, either formed at the surface or even fallen down (as we suppose) from the plasma volume. The dominating abundance of horizontally packed nanotubes over the column top surface (Fig. 5c) probably indicates that the electric field effect at the open end of a nanotube [6,17] is not a governing factor for its growth. Those nanotubes (Fig. 5c) that were originally located near the very hot top of a hemisphere could then undergo evaporation, yielding neutral carbon particles. An estimate has shown [6] that the majority of carbon precipitated on columns must evaporate back as neutrals. This evaporation enriches the central part of a column in nanoparticles and graphite to the extent finally observable with the SEM (Fig. 6b), as these components are thermodynamically more stable compared to nanotubes [17]. At the periphery of a column the evaporation is less effective and nanotubes mostly survive, thereby forming the braid of a column (Fig. 7a and Fig. 8). Obviously nonreactive helium carries re-evaporated carbon neutrals to zone 2, where they serve as a principal feedstock for the growth of new nanotubes [6].

Because of the existence of columnar structures with a low nanotube concentration it is evident that the presence of nanotubes may not be vital for column formation in the deposits. It can be supposed that nanotubes grow in preference on columns just because of favorable conditions for their growth there, for example a suitable temperature range at the growth surfaces. Nevertheless, when formed nanotubes probably stimulate more regular and stable column formation, since nanotube rich deposits generally have a more explicit and regular columnar structure, as compared to cases of low nanotube concentration. The reciprocal influence of columns and nanotubes needs further exploration.

As has been found, nanotubes were most abundant in the intercolumnar space and in the braids of columns (Fig. 7a, Figs. 8 and 9), and this may serve as a hint for developing the technique for their separation and purification. Besides this, the structures of zone 1 and zone 2 disclosed in this work give an explanation for the generally irreproducible results of repeated TEM analysis of the composition of differently prepared samples of the core material.

From the conclusion (based on the fractal character of columnar structures) that columnar deposit formation and nanotube growth take place in a nonlinear process in the arc plasma, several important things for the deposit growth come out: (1) almost all the parameters of the arcing process are interdependent; an attempt to adjust only one of them will lead to inevitable variation of others; (2) no sole parameter or its value can be regarded as the most

nological result (for example high nanotube yield) could be achieved; (3) several sets of controllable parameters can give similar results; (4) not all the sets of experimental parameters provide stable growth. Sometimes oscillations of growth processes can take place and periodic changes of the structure in the deposits can be observed: for example, along the deposit axis loose columnar structures can be periodically displaced by dense sliced structures and vice versa. As it is not productive to stabilize growth processes in unstable domains of the growth, it is of prime importance to find these islands of stability in the ocean of possible experimental parameters for appropriate deposit production [5–12,18]. The conditions listed in Table 1 illustrate important solutions in our search for better production of nanotubes.

5. Conclusions

With the help of a thorough electron microscopical investigation, using both TEM and SEM techniques, we have clarified the main peculiarities of the columnar structures of the nanotube-rich deposits prepared under stable arcing conditions. Taking into consideration these newly observed peculiarities (the absence of co-oriented longitudinal nanotubes or their bundles and the preferential orientation of nanotubes in column coverings at high angles to the deposit axis) the refined stationary model of deposit growth has been outlined, that is in accordance with our observations by electron microscopy. These peculiarities might be helpful in the explanation of existing confusion that arises because of the effects of deposit preparation and further sample handling.

Acknowledgements

N.K. is grateful to Dr. J.L. Hutchison for HREM investigations. The use of the facility at the Max-Planck many) is greatly appreciated. This work has been fulfilled under the financial support of 079 ISTC Project.

References

[1] Rinzler AG, Hafner JH, Nikolaev P, Lou L, Kim SG, Tomanek D, Nordlander P, Colbert DT, Smalley RE. Science 1995;269:1550.

[2] deHeer WA, Chatelain A, Ugarte D. Science 1995;270:1179.

[3] Iijima S, Ichihashi T, Ando Y. Nature 1992;356:776.

[4] Ebbesen TW, Hiura H, Fujita J, Ochiai Y, Matsui S, Tanigaki K. Chem Phys Lett 1993;209:83.

[5] Wang XK, Lin XW, Song SN, Dravid VP, Ketterson JB, Chang RPH. Carbon 1995;33:949.

[6] Colbert DT, Zhang J, McClure SM, Nikolaev P, Chen Z, Hafner JH, Owens DW, Kotula PG, Carter CB, Weaver JH, Rinzler AG, Smalley RE. Science 1994;266:1218.

[7] Hiura H, Ebbesen TW, Tanigaki K. Adv Mater 1995;7:273.

[8] Iijima S. Nature 1991;354:56.

[9] Saito Y, Yoshikawa T, Inagaki M, Tomita M, Hayashi T. Chem Phys Lett 1993;204:277.

[10] Seraphin S, Zhou D, Jiao J, Withers JC, Loutfy R. Carbon 1993;31:685.

[11] Ajayan PM, Stephan O, Colliex C, Trauth D. Science 1994;265:1212.

[12] Wang XK, Lin XW, Dravid VP, Ketterson JB, Chang RPH. Appl Phys Lett 1993;62:1881.

[13] Kotosonov AS, Kuvshinnikov SV. Phys Lett A 1997;A240:377.

[14] Krestinin AV, Moravsky AP. Chem Phys Lett 1998;286:479.

[15] Mandelbrot BB. Fractal geometry of nature. San Francisco: Freeman, 1982.

[16] Briggs J. Fractals, the patterns of chaos. London: Thames and Hudson, 1992.

[17] Smalley RE. Mater Sci Eng 1993;B19:1.

[18] Taylor GH, Fitz Gerald JD, Pang L, Wilson MA. J Crystal Growth 1994;135:157.